Environmental Pollution 388 (2026) 127347

Contents lists available at ScienceDirect

Environmental Pollution

journal homepage: www.elsevier.com/locate/envpol

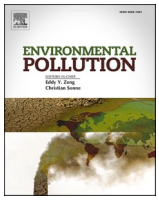

PM_{10} chemical fingerprints and source assessment guiding air quality improvements by 2030 in Andalusia, southern Spain☆

Pablo Pérez-Vizcaíno [a,b,*], Ana M. Sánchez de la Campa [a,b], Daniel Sánchez-Rodas [a,c], Andrés Alastuey [a,d], Xavier Querol [a,d], Jesús D. de la Rosa [a,b]

[a] Associate Unit CSIC-University of Huelva "Atmospheric Pollution", Center for Research in Sustainable Chemistry – CIQSO, University of Huelva, E21007, Huelva, Spain
[b] Department of Earth Sciences, Faculty of Experimental Sciences, University of Huelva, Campus El Carmen s/n, E21007, Huelva, Spain
[c] Department of Chemistry, Faculty of Experimental Sciences, University of Huelva, Campus El Carmen s/n, E21007, Huelva, Spain
[d] Institute of Environmental Assessment and Water Research (IDAEA-CSIC), 08034, Barcelona, Spain

ARTICLE INFO

Keywords:
Air pollution
Air quality policy
Air quality standards
Receptor modelling
Source apportionment

ABSTRACT

This study focuses on the evaluation of 2021–2023 PM_{10} concentrations, chemical speciation and source apportionment (with receptor modelling) of samples collected at 21 air quality monitoring stations (urban, urban-industrial, traffic hotspots and rural) from Andalusia (southern Spain). After subtracting the natural dust contribution, 9/21 sites would exceed the annual PM_{10} limit value of 20 μg m^{-3} set by the new Ambient Air Quality Directive (EU) 2024/2881. Source apportionment analysis carried out with PMF identified six major sources of PM_{10}: Crustal, Marine, Combustion (biomass burning and traffic mix), Traffic, Regional and Industrial. The main anthropogenic source was Combustion, with the exception of those stations located in cities with a high road traffic density, where Traffic was the dominant anthropogenic source. To comply with the objectives of the Directive (EU) 2024/2881, a reduction of 5–50 % in anthropogenic sources is proposed, based on the sum of their interannual mean concentrations at the nine potentially non-compliance sites. The study evidences the complexity of separating specific source contributions of PM_{10}, highlighting the need to conduct higher time resolution studies to better identify and quantify source contributions and their temporal variations, as well as the need to combine deterministic and receptor modelling for a complete source apportionment, specially of secondary PM contributions.

1. Introduction

Particulate matter (PM) is a common proxy indicator for air pollution, currently considered one of the main environmental threats to human health (World Health Organization, 2021; Chowdhury et al., 2022; Marquès et al., 2022; Mebrahtu et al., 2023). A significant number of clinical and epidemiological studies have reported that exposure to air pollution increases mortality due to cardiovascular (e.g., Peters, 2005; Polichetti et al., 2009; Martinelli et al., 2013) and respiratory (e.g., Neuberger et al., 2004; Weinmayr et al., 2010; Jo et al., 2017) diseases. PM is characterized by its complex physicochemical properties and source contributions, both natural and anthropogenic (Moreno et al., 2006).

Given the consistent association between PM and health outcomes, the European Commission adopted the Directive 1999/30/EC, which included an annual (40 μg m^{-3}) limit value for PM_{10} (particles whose aerodynamic diameter is equal to or less than 10 μm) (European Commission, 1999). This value was kept in the subsequent air quality standard 2008/50/EC (European Commission, 2008). In 2021, an annual limit value of 15 μg m^{-3} for PM_{10} was recommended (World Health Organization, 2021). In view of this recommendation, the new Ambient Air Quality Directive (EU) 2024/2881, which came into force in December 2024, set an annual PM_{10} limit value of 20 μg m^{-3} (European Union, 2024). The compliance with this limit will be required since January 1st, 2030.

On a global scale, policies have been implemented to improve air

☆ This paper has been recommended for acceptance by Prof. Pavlos Kassomenos.

* Corresponding author. Associate Unit CSIC-University of Huelva "Atmospheric Pollution", Center for Research in Sustainable Chemistry – CIQSO, University of Huelva, E21007, Huelva, Spain.
E-mail address: pablo.perez@ciqso.uhu.es (P. Pérez-Vizcaíno).

https://doi.org/10.1016/j.envpol.2025.127347
Received 30 July 2025; Received in revised form 11 October 2025; Accepted 2 November 2025
Available online 4 November 2025

quality due to the encouragement of authorities and civil society to increase efforts to control and study the harmful effects of exposure to air pollution. One of the main hotspots, China, reduced its anthropogenic PM_{10} emissions by approximately 40 % between 2010 and 2017 (Zheng et al., 2018). However, despite these improvements, the global impact in deaths and years of healthy life lost has barely decreased since the 1990s (World Health Organization, 2021). In Europe, there is a consistent decreasing trend of the mean annual PM_{10} concentrations along the last two decades (European Environment Agency, 2024). Nevertheless, it is estimated that in different regions of Europe, including Spain, Italy and other southern and eastern European regions, there will be a high probability of non-compliance for the forthcoming new annual limit value (Beloconi and Vounatsou, 2023). For this reason, it is crucial to analyze the current source contributions to PM_{10} in order to assess cost-effective abatement strategies. A useful tool for this purpose is the Positive Matrix Factorization (PMF v5.0 EPA) receptor model (Paatero and Tapper, 1994). This receptor modelling tool allows the identification of sources through chemical profiles and the quantification of the contribution of each one based on PM chemical speciation datasets obtained at receptor sites. PMF is a more stable and robust receptor modelling tool compared to other models (Cesari et al., 2016a; Belis et al., 2019). In addition, the Research Infrastructures Services Reinforcing Air Quality Monitoring Capacities in European Urban & Industrial AreaS (RI-URBANS, 2025) recently provided 16 advanced service tools to meet the demands of new and complex urban air quality scenarios and enhance the analysis of air quality. One of these service tools consisted of a methodology for source apportionment receptor modelling in which PMF was recognized as the most widely used receptor model (RI-URBANS-ST10, 2025).

In recent years, numerous studies aimed at assessing the source contributions to PM in relation to air quality assessment in port areas (i.e., Pérez et al., 2016; Clemente et al., 2021), industrial estates (i.e., Cesari et al., 2016b; Li et al., 2018) and urban environments (i.e., Gupta et al., 2012; Amato et al., 2014; Sharma et al., 2014; Liu et al., 2025a). However, most of these works are based on a limited number of monitoring stations and cover time periods of approximately one year. Short-term studies do not take into account the wide variability of meteorological scenarios that may occur or the impact of different sources. This causes a loss of information on seasonal variations, weaker representativeness, difficulty in identifying long-term trends, and less robust spatial comparisons. These disadvantages are solved considering instead long-term and multi-site studies. Despite this scarcity of long-term studies, some steps have already been taken to abate PM_{10} levels and improve air quality, mostly based on assessments derived from emission inventories and deterministic modelling tools. In the case of road traffic, congestion charges and low emission zones (LEZs) have been implemented in several European cities, restricting the access and circulation of vehicles (e.g., Holman et al., 2015; Santos et al., 2019; Zhai and Wolff, 2021; Gu et al., 2022). The limit for sulphur content of fuel oil for ships has been reduced to 0.5 % following the rule IMO 2020. The implementation of successive EURO1/I to 6/VI vehicle emission standards, and of the directives on industrial emissions, have considerably reduced PM concentrations (i.e., in ′t Veld et al., 2021). All this policy actions have prompted in a decrease of PM_{10} across Europe (with some regions succeeding more than others, European Environment Agency, 2024). Accordingly, continued efforts to reduce PM_{10} are needed, although this is currently more complex than in previous decades, as the largest fraction of PM is of secondary origin (i.e., in ′t Veld et al., 2021).

This study provides an evaluation of PM_{10} concentrations, chemical speciation, and source contribution in Andalusia, southern Spain, a highly populated region characterized by complex orography, during 2021–2023. A receptor-modelling source apportionment analysis with PMF was carried out with samples from 21 air quality monitoring stations (urban, urban-industrial, traffic hotspots and rural) distributed throughout the region to assess on the origin of PM_{10} at each one. The aim of the study was to understand the regional and temporal variability in source contributions, and to propose abatement strategies, especially for these cities with a high 2030 non-compliance potential for PM_{10}. The main contribution of this study is the implementation of receptor modelling source apportionment based on the evaluation of long-term PM_{10} speciation datasets to assess on the strategies needed to attain compliance with the PM_{10} standard of the Ambient Air Quality Directive (EU) 2024/2881 to be met from January 1st, 2030.

2. Study area

Andalusia is the most populated (ca. 8.4 M inhabitants) autonomous region of Spain and the second largest in extension (ca. 88 000 km^2). Its complex orography is dominated by the mountain systems of Sierra Morena to the north, and the Betic Ranges to the south (Fig. 1). In the latter, the highest altitude of the Iberian Peninsula (3478 m a.s.l.) is located. Both systems are separated by a NE-SW oriented topographic depression, the Guadalquivir Valley (ca. 650 km in length).

Andalusia has a dominant Mediterranean climate, with mild winters, irregular precipitation, and warm and dry summers. Due to its large extension and complex topography, other microclimates such as desert and highland climates, locally occur in Andalusia. The region is geographically located in the southwest of Europe and very close to the North African coast (Fig. 1), so it is also affected by the impact of frequent high African dust air masses crossing Europe (Rodríguez et al., 2001; Salvador et al., 2022).

Andalusia has traditionally been an agricultural region, especially in the Guadalquivir Valley area. Nevertheless, from the 60s and 70s, tourism became a key economic factor. Another important sector, although with less relevance to the local economy, is industry. Two major areas related to the chemical and petrochemical industries have been extensively studied in prior campaigns: the Bay of Algeciras (e.g., Moreno et al., 2010; Pandolfi et al., 2011; Li et al., 2018) and the Estuary of Huelva (e.g., Querol et al., 2002; Alastuey et al., 2006; Sánchez de la Campa et al., 2018; Millán-Martínez et al., 2021a). Some towns in Jaén have developed an important ceramic industry and/or biomass burning processes over the years (e.g., Sánchez de la Campa et al., 2010; Pérez-Pastor et al., 2020). Finally, in some metropolitan areas of Andalusia (Granada, Málaga and Seville), pollution hotspots related to significant urban road traffic have also been identified (de la Rosa et al., 2010).

3. Methodology

3.1. Sampling locations

The 21 air quality monitoring stations considered in this study are distributed among the 8 provinces into which Andalusia is divided: Almería, Granada, Jaén and Málaga (eastern Andalusia), Cádiz, Córdoba, Huelva and Seville (western Andalusia). The monitoring sites selected cover different types of environments, including the following ones (Table S1).

- **Urban** (8 stations): Alcalá de Guadaíra, Lepanto, Mediterráneo, Palacio de Congresos, Plaza Castillo, Ronda del Valle, San Fernando and Villanueva del Arzobispo.
- **Urban-Industrial** (7 stations): Bailén, Campus, La Línea, La Rábida, Los Barrios, Moguer and Puente Mayorga.
- **Traffic** (4 stations): Carranque, Granada Norte, Príncipes and Torneo.
- **Rural** (2 stations): Matalascañas and Sierra Norte.

The urban monitoring stations are located in large population centers (Córdoba, Almería, Granada and Jaén). The urban site of Villanueva del Arzobispo stands out for the high levels of PM associated with biomass burning emissions from the use of olive waste as biofuel for

Fig. 1. Map with the location of the 8 most important cities in Andalusia (black circles) and the 21 monitoring stations considered in this study, classified as: Urban: blue circle; Urban-Industrial: green triangle; Traffic: red star; Rural: yellow square. (For interpretation of the references to colour in this figure legend, the reader is referred to the Web version of this article.)

domestic heating (Pérez-Pastor et al., 2020). The urban-industrial sites are located near the industrial areas of the Bay of Algeciras (La Línea, Los Barrios and Puente Mayorga) and the Estuary of Huelva (Campus, La Rábida and Moguer). In the case of Bailén station, high concentrations of SO_2, PM and other elements associated with the ceramic industry and the burning of pine and olive husk (K, Ni, Rb and V), have been measured (de la Rosa et al., 2010; Sánchez de la Campa et al., 2010). Regarding rural stations, Matalascañas is located about 40 km from the industrial area of the Estuary of Huelva, so it may be influenced by industrial emissions from the activities carried out there. Sierra Norte station is located far from any major population center, so it is not affected by nearby anthropogenic emissions. Traffic monitoring sites are located in areas with a significant density of vehicles within heavily populated cities: Príncipes and Torneo (Seville), Carranque (Málaga) and Granada Norte (Granada). At these traffic hotspots, high levels of PM_{10} and gaseous pollutants (CO and NO_2) have been reported (de la Rosa et al., 2010; Amato et al., 2014; Fernández-Camacho et al., 2016; Millán-Martínez et al., 2021b; Piscitello et al., 2021).

3.2. PM_{10} sampling and chemical analysis

Offline PM_{10} sampling was performed using manual gravimetric MCV or DIGITEL high-volume (30 $m^3\ h^{-1}$) or low-volume (2.3 $m^3\ h^{-1}$) samplers equipped with MUNKTELL quartz fiber filters. The sampling frequency was one daily filter (24-h) every 6 days. A total of 3722 daily samples were collected between 2021 and 2023 using this procedure. After sampling, filters were placed in a constant temperature and relative humidity (20 ± 1 °C and 50 ± 5 %, respectively) room. The gravimetric analysis of blank and sampled filters was performed in this room using a Sartorius LA130S-F balance (0.1 mg sensitivity). The standard method UNE-EN 12341 (UNE-EN 12341, 2024) was followed.

For chemical analysis, a half of each filter was digested in acidic medium (2.5 mL HNO_3: 5 mL HF: 2.5 mL $HClO_4$) following the method proposed by Querol et al. (2002). Determination of the contents of major elements was performed using ICP-OES (Agilent 5110), and trace elements by using ICP-MS (Agilent 7900). For quality control, analysis of NIST-1663b (fly ash, Standard Reference Material) was conducted during every analytical run of both ICP techniques. External calibration was performed in ICP-MS by using cocktail solutions (1, 10, 50, 100 and 250 ppb as well as a HNO_3 5 % blank). The external calibration for ICP-OES was performed using elemental standards solutions (0.05–100 ppm and a HNO_3 5 % blank). More detailed information on controls and calibration can be found in Millán-Martínez et al. (2021a). The average precision and accuracy fall for most of the elements under the typical analytical errors (in the range of 5–10 %), and were controlled by repeated analysis of NBS-1633c (fly ash) reference material.

The soluble fraction of a 1/4 of each filter was extracted with Milli-Q grade deionized water at 60 °C and the content of major anions (Cl^-, F^-, NO_3^- and SO_4^{2-}) and NH_4^+ in the leaches was determined by ion chromatography (Metrohm 883 Basis IC plus). The accuracy and detection limit were 10 % and 0.4 μg m^{-3} (Millán-Martínez et al., 2021a). A 1.5 cm^2 rectangular portion of each filter was used to determine elemental and organic carbon (EC and OC, respectively) with thermo-optical method (Sunset Lab Analyzer) using the EUSAAR_2 protocol (Cavalli et al., 2010).

SiO_2 and CO_3^{2-} concentrations were indirectly determined from the contents of Al, Ca, and Mg, on the basis of experimental equations ($3*Al_2O_3 = SiO_2$; $1.5*Ca + 2.5*Mg = CO_3^{2-}$) (Querol et al., 2001). Levels of SO_4^{2-} anthropogenic were obtained by subtracting the SO_4^{2-} marine (indirectly determined by stoichiometry from the soluble Na levels) from $SO_{4\,total}^{2-}$ (Querol et al., 2002). The chemical components were grouped as follows: a) Mineral (sum of CO_3^{2-}, SiO_2, Al_2O_3, Ca, Fe, K and PO_4^{3-}); b) Sea Salt (sum of Na, Mg, F^-, SO_4^{2-} marine and Cl^-); Secondary Inorganic Compounds (SIC, sum of SO_4^{2-} anthropogenic, NO_3^- and NH_4^+); and d) Total Carbon (TC, sum of OC and EC).

3.3. Receptor model

The goal of receptor models is to solve the chemical mass balance between measured species concentrations and sources profiles. In this

study, the Positive Matrix Factorization model (PMF v5.0 EPA) was used as the method for estimating sources identification and contributions. The method is described in greater detail in Paatero and Tapper (1994) and Paatero (1997). PMF is a multivariate factor analysis tool that decomposes a matrix of speciated sample data (X) of i by j dimensions into two matrices: factor contributions (G) and factor profiles (F). The model is based on the following equation:

$$X_{ij} = \sum_{k-1}^{p} G_{ik} * F_{kj} + E_{ij} \quad \text{(eq. 1)}$$

where i is the number of samples and j the chemical species measured. The number of factors is expressed by p. G_{ik} is the contribution of each source to each sample, F_{kj} represents the concentration of the species from each source and E_{ij} is the residual for each sample/species.

PMF uses both sample concentration and user-provided uncertainty associated with the sample data to weight individual points. The number of species selected in the PMF was chosen based on their signal-to-noise ratio (S/N) (Paatero and Hopke, 2003). Those elements with an S/N value > 2.2 were classified as "strong", those with $0.2 < S/N < 2.2$ as "weak", and those with $S/N < 0.2$ as "bad". These last elements are not considered in the model. The species considered in the source apportionment analysis from the 21 monitoring stations were Al, Ca, K, Na, Mg, Fe, Mn, Ti, PO_4^{3-}, Zn, Sr, Pb, SO_4^{2-}, NO_3^-, Cl^-, NH_4^+, OC and EC. Other species were taken into account or not according to each station (Table S2).

4. Results and discussion

4.1. Levels of PM_{10} during the study period

The 2021–2023 mean of PM_{10} concentrations reached 17.9–31.8 μg m^{-3} at urban sites, 18.7–30.1 μg m^{-3} at urban-industrial sites, 24.0–29.9 μg m^{-3} at traffic sites, and 18.6–22.3 μg m^{-3} at rural sites. In 18/21 sites, PM_{10} annual mean exceeded the forthcoming (2030) new limit value of 20 μg m^{-3} (Fig. 2 and Table S3). The site with the highest PM_{10} concentration mean was Villanueva del Arzobispo (31.8 μg m^{-3}). This urban station was also the one with the maximum annual mean levels in 2021 (33.4 μg m^{-3}) and 2023 (31.1 μg m^{-3}), while for 2022 it was the Torneo traffic station (36.3 μg m^{-3}) (Table S3).

The above ranges are lower than those previously measured by Millán-Martínez et al. (2021b) at some of these monitoring sites for the period 2007–2014. These latter ranges were already lower than those reported by de la Rosa et al. (2010) for Andalusia in 2007. This downward trend is particularly noticeable in urban-industrial and traffic monitoring sites. The decrease is attributed to reductions of PM (and gaseous precursors) emission abatements associated to the above European, national, regional and local policy actions implemented (i.e., Querol et al., 2014; Li et al., 2018; Sánchez de la Campa et al., 2018; in 't Veld et al., 2021).

4.2. PM_{10} net load of African dust

As previously mentioned, PM_{10} concentrations in Andalusia are frequently affected by outbreaks of high African dust air masses, given its proximity to the African continent (around 30 % of the days, with 3.0–4.3 μg m^{-3} annual contribution, as averages for 2001–2016, Querol et al., 2019). These natural PM contributions are allowed to be subtracted from daily and annual means for the evaluation of compliance with the Ambient Air Quality Directive (EU) 2024/2881 (European Union, 2024). The procedure recommended by the European Commission (2011) has been used in this study.

Firstly, two regional background stations were selected: Barcarrota (for western Andalusia) and Viznar (for eastern Andalusia). More

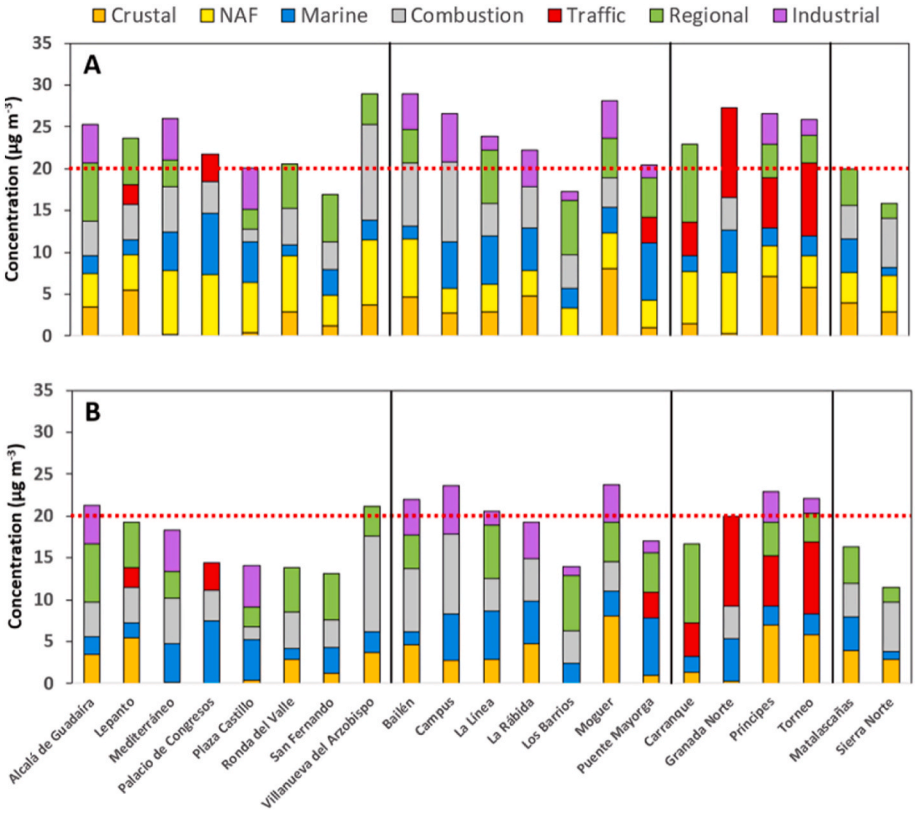

Fig. 2. Bar plots of the concentration of each source identified for each monitoring station in this study including the North African dust load (NAF) (A) and excluding it (B). The red dotted line represents the limit of 20 μg m^{-3} set by the new Ambient Air Quality Directive (EU) 2024/2881. (For interpretation of the references to colour in this figure legend, the reader is referred to the Web version of this article.)

information on both can be found in Escudero et al. (2007). Subsequently, the 40th percentile was subtracted from the daily value of PM_{10} on those days in which African dust events occurred at Barcarrota and Viznar stations (as detected by the output of the modelling tools refereed by European Commission, 2011). The difference between the daily PM_{10} levels measured at both stations and the daily PM_{10} levels calculated using this methodology represents the net PM_{10} African dust load.

In 2021–2023, the PM_{10} African dust load ranged between 3.0 and 4.3 μg m^{-3} for stations located in western Andalusia (similar to the range given by Querol et al., 2019) and between 6.0 and 7.7 μg m^{-3} in eastern Andalusia (higher than the range mentioned) (Table S3). This load represented more than 34 % of the concentration of the crustal contribution (determined by chemical speciation) in western and eastern Andalusia. The year in which the highest concentration of PM_{10} African dust was measured was 2022 (Fig. S1). By subtracting the contribution of PM_{10} African dust, the forthcoming annual limit value of 20 μg m^{-3} would have been exceeded in 9/21 sites (Alcalá de Guadaíra, Villanueva del Arzobispo, Bailén, Campus, La Línea, Moguer, Granada Norte, Príncipes and Torneo), as opposed to the 18/21 before the subtraction (Table 1, Fig. 2 and Table S3).

4.3. PM_{10} major components

The major PM species were grouped into four components: Mineral, Sea Salt, SIC and TC. (Table 2). Information on the mean concentration of each species in each year at the 21 monitoring sites are reported in Tables S4–S6.

The sum of the chemical components of PM_{10} for each monitoring site is depicted in Fig. 3. In general, the highest variability was observed at urban and urban-industrial monitoring stations. Rural stations clearly showed the lowest mean values of the SIC and TC components. The mean concentration of the Mineral component (CO_3^{2-}, SiO_2, Al_2O_3, Ca, Fe, K and PO_4^{3-}) for the period 2021–2023 reached 5.5–16.7 μg m^{-3} at urban sites, 5.0–14.6 μg m^{-3} at urban-industrial sites, 9.3–14.6 μg m^{-3} at traffic sites, and 8.3–10.2 μg m^{-3} at rural sites (Fig. 3). This component represented between 49 and 55 % of the annual PM_{10} concentrations. The site with the highest mean concentration was the Palacio de Congresos urban site (16.7 μg m^{-3}) in Granada. The maximum annual mean was also reached at this station (20.8 μg m^{-3}) in 2022 (Fig. S2) where this component represented the 71 % of the total PM_{10} concentration. This high percentage was due to the fact that, in March of that year, Granada was one of the Andalusian regions most affected by two episodes of extreme African air masses outbreaks across Europe (e.g., Cuevas-Agulló et al., 2024; Rodríguez and López-Darias, 2024). At the Granada Norte traffic station, a high value of the Mineral component was also measured in 2021–2023 (15.8 μg m^{-3}; 62 % of the total PM_{10} concentration). Other mineral contributions with high load of calcite ($CaCO_3$) and dolomite ($CaMg(CO_3)_2$), enriched in the soils and rocks of some parts of Andalusia (e.g., López-Quirós et al., 2016), could also have contributed to increasing Mineral component.

The Sea Salt (Na, Mg, F^-, SO_4^{2-} marine and Cl^-) concentrations reached 1.2–5.1 μg m^{-3} at urban sites, 1.4–4.6 μg m^{-3} at urban-industrial sites, 1.5–3.0 μg m^{-3} at traffic sites, and 1.2–3.7 μg m^{-3} at rural sites (Fig. 3). The relative contribution of Sea Salt reached 10–15 % of the total PM_{10}. Maximum concentrations were measured at stations located on the Atlantic (San Fernando and Matalascañas stations) or the Mediterranean (Carranque, La Línea, Mediterráneo, Plaza Castillo and Puente Mayorga stations) coast. In 2021, this component came to represent up to 30 % of the total PM_{10} concentration at Plaza Castillo urban station (5.8 μg m^{-3}; Fig. S2). It is also relevant to mention that Sea Salt can be also considered as a natural PM_{10} contribution according to European Commission (2011), and consequently subtracted from measured PM_{10} for compliance purposes.

SIC (SO_4^{2-} anthropogenic, NO_3^- and NH_4^+) mean concentrations reached 2.8–4.2 μg m^{-3} at urban sites, 3.1–5.8 μg m^{-3} at urban-industrial sites, 3.5–4.0 μg m^{-3} at traffic sites, and 2.0–2.9 μg m^{-3} at rural sites (Fig. 3). The mean relative contribution to PM_{10} reached 15–20 %. The site with the highest mean concentration was La Línea (5.8 μg m^{-3}) and the second was Puente Mayorga station (4.4 μg m^{-3}), both located in the province of Cádiz (Fig. 1). Maximum annual mean

Table 1
Interannual (2021–2023) mean concentration (μg m^{-3}) of each source identified at each monitoring station (Urban: UB; Urban-Industrial: UB-IN; Traffic: TR; Rural: RU). The contribution of the North African dust load (NAF) has been indicated. Stations that exceeded the PM_{10} limit of the new directive (20 μg m^{-3}) have been indicated in red. In a bold box, the main anthropogenic activities of each station are highlighted (see text).

				μg m^{-3}								
Monitoring station	**Province**	**Type**	**Samples**	**PM_{10}**	**Crustal**	**NAF**	**Marine**	**Combustion**	**Traffic**	**Regional**	**Industrial**	**Total**
Alcalá de Guadaíra	Seville	UB	168	25.5	3.4	**4.0**	2.1	4.2	0.0	7.0	4.5	21.2
Lepanto	Córdoba	UB	182	25.5	5.4	**4.3**	1.8	4.3	2.3	5.5	0.0	19.3
Mediterráneo	Almería	UB	173	26.5	0.1	**7.7**	4.7	5.4	0.0	3.2	4.9	18.3
Palacio de Congresos	Granada	UB	184	24.9	0.0	**7.3**	7.4	3.7	3.3	0.0	0.0	14.5
Plaza Castillo	Almería	UB	178	22.4	0.4	**6.0**	4.8	1.6	0.0	2.4	4.9	14.1
Ronda del Valle	Jaén	UB	169	22.2	2.8	**6.7**	1.4	4.3	0.0	5.4	0.0	13.9
San Fernando	Cádiz	UB	174	17.9	1.2	**3.7**	3.1	3.2	0.0	5.6	0.0	13.2
Villanueva del Arzobispo	Jaén	UB	181	31.8	3.7	**7.7**	2.4	11.4	0.0	3.6	0.0	21.2
Bailén	Jaén	UB-IN	182	30.1	4.7	**7.0**	1.5	7.6	0.0	3.9	4.3	22.0
Campus	Huelva	UB-IN	187	28.8	2.8	**3.0**	5.5	9.5	0.0	0.0	5.8	23.6
La Línea	Cádiz	UB-IN	159	21.7	2.8	**3.3**	5.8	3.9	0.0	6.4	1.6	20.6
La Rábida	Huelva	UB-IN	174	24.2	4.8	**3.0**	5.1	5.0	0.0	0.0	4.4	19.3
Los Barrios	Cádiz	UB-IN	164	18.7	0.0	**3.3**	2.3	4.0	0.0	6.6	1.1	14.0
Moguer	Huelva	UB-IN	180	28.6	8.0	**4.3**	3.0	3.5	0.0	4.8	4.5	23.8
Puente Mayorga	Cádiz	UB-IN	201	21.9	1.0	**3.3**	6.8	0.0	3.1	4.7	1.5	17.1
Carranque	Málaga	TR	182	24.0	1.4	**6.3**	1.9	0.0	4.0	9.4	0.0	16.7
Granada Norte	Granada	TR	180	28.8	0.3	**7.3**	5.1	3.9	10.7	0.0	0.0	20.0
Príncipes	Seville	TR	179	27.1	7.1	**3.7**	2.2	0.0	6.0	4.1	3.6	22.9
Torneo	Seville	TR	154	29.9	5.9	**3.7**	2.4	0.0	8.7	3.3	1.9	22.2
Matalascañas	Huelva	RU	189	22.3	3.9	**3.7**	3.9	4.1	0.0	4.4	0.0	16.4
Sierra Norte	Seville	RU	182	18.6	2.9	**4.3**	1.0	6.0	0.0	1.7	0.0	11.5
Mean (μg m^{-3})				24.8	3.0	**4.9**	3.5	4.1	1.8	3.9	2.0	18.4

Table 2
Interannual (2021–2023) mean concentration of major components (μg m^{-3}) and trace elements (ng m^{-3}) for each group of stations (Urban, Urban-Industrial, Traffic and Rural). LOD: Limit of Detection.

Major components				
μg m^{-3}	Urban	Urban-Industrial	Traffic	Rural
C_{total}	4.0	3.2	4.8	2.7
OC	3.3	2.6	3.6	2.4
EC	0.7	0.6	1.2	0.3
CO_3^{2-}	3.2	2.4	3.3	2.1
SiO_2	4.2	3.7	4.5	3.9
Al_2O_3	1.4	1.2	1.5	1.3
Ca	1.5	1.1	1.6	1.0
K	0.5	0.4	0.4	0.4
Na	1.0	1.2	0.9	1.0
Mg	0.4	0.3	0.4	0.3
Fe	0.5	0.5	0.8	0.4
PO_4^{3-}	0.1	0.1	0.1	0.1
$SO_{4\,total}^{2-}$	1.7	2.0	1.7	1.5
F^-	<LOD	0.1	<LOD	0.1
SO_4^{2-} anthropogenic	1.4	1.7	1.5	1.2
SO_4^{2-} marine	0.3	0.3	0.2	0.3
NO_3^-	1.7	1.7	1.8	1.1
Cl^-	0.9	1.0	0.7	0.9
NH_4^+	0.2	0.4	0.3	0.2
Mineral	11.4	9.4	12.1	9.2
Sea Salt	2.6	2.9	2.2	2.5
SIC	3.3	3.8	3.5	2.4
TC	4.0	3.2	4.8	2.7
Trace elements				
ng m^{-3}	**Urban**	**Urban-Industrial**	**Traffic**	**Rural**
Li	0.5	0.5	0.5	0.5
Be	0.1	0.1	0.1	0.1
Sc	0.1	0.1	0.2	0.1
Ti	50.5	51.3	66.0	44.6
V	2.6	6.9	3.5	1.9
Cr	2.5	6.0	4.5	1.7
Mn	8.3	8.8	11.3	9.0
Co	0.2	0.3	0.3	0.2
Ni	2.6	6.0	3.0	2.2
Cu	9.0	63.3	16.3	3.8
Zn	27.9	36.5	28.2	20.8
Ga	0.2	0.2	0.3	0.2
Ge	0.2	0.2	0.2	0.2
As	0.4	2.1	0.6	0.8
Se	0.1	0.1	0.1	0.1
Rb	0.1	1.1	1.2	1.1
Sr	5.5	3.9	5.9	3.3
Y	0.5	0.4	0.5	0.4
Zr	1.8	1.8	2.2	1.5
Nb	0.2	0.2	0.2	0.1
Mo	3.5	3.1	3.5	3.0
Cd	0.1	0.4	0.1	0.1
Sn	1.4	1.1	3.3	0.7
Sb	0.8	0.7	1.7	0.3
Cs	0.1	0.1	0.1	0.1
Ba	14.0	11.6	21.1	9.1
La	0.5	0.7	0.6	0.4
Ce	1.0	0.8	1.1	0.8
Pb	4.6	12.7	5.8	4.0
Bi	0.7	0.4	0.4	0.1
Th	0.1	0.1	0.1	0.1
U	0.1	0.1	0.1	0.1

was also reached at La Línea urban-industrial station (8.7 μg m^{-3}; 40 %) in 2021 (Fig. S2). High values of this component in urban-industrial stations are expected due, among others, to SO_4^{2-} emissions of anthropogenic origin from fuel oil combustion from shipping in areas such as the Bay of Algeciras and the Strait of Gibraltar (Pandolfi et al. 2011).

The TC (OC + EC) concentrations reached 2.2–7.3 μg m^{-3} (OC/EC ranged between 3.1 and 5.7) at urban sites, 2.1–5.4 μg m^{-3} (OC/EC ranged between 3.1 and 6.5) at urban-industrial sites, 3.5–6.0 μg m^{-3} (OC/EC ranged between 2.5 and 4.6) at traffic sites, and 2.4–3.0 μg m^{-3} (OC/EC ranged between 6.9 and 11.8) at rural sites (Fig. 3). The relative contribution of TC to bulk PM_{10} reached 16–21 %. The station with the highest TC (7.6 μg m^{-3}, OC/EC reached 5.4) and OC (6.4 μg m^{-3}) concentrations was the Villanueva del Arzobispo site, due to the widespread biomass combustion processes in that area (Pérez-Pastor et al., 2020). Maximum annual mean was also reached at this station (8.2 μg m^{-3}) in 2021 (Fig. S2) where TC reached the 29 % of the total PM_{10} concentration. However, when considering the average for the group of sites, traffic sites showed the highest mean of this component (Table 2 and Fig. 3) due to PM exhaust emissions (Amato et al., 2014; Piscitello et al., 2021). The Granada Norte and Torneo traffic sites were the stations with the highest concentration of EC (1.7 μg m^{-3} and 1.5 μg m^{-3}, respectively).

4.4. Trace elements

As it could be expected, the highest 2021–2023 loads of metals associated with metallurgical activity were measured at urban-industrial sites (Table 2). Particularly, the maximum mean concentration of As (6.6 ng m^{-3}), Cd (0.8 ng m^{-3}), Cu (242.7 ng m^{-3}) and Pb (32.3 ng m^{-3}) were measured at La Rábida station (Tables S4–S6). As has been reported in prior studies (e.g., Fernández-Camacho et al., 2010), these elements are associated with the emissions from a copper smelter located in the Estuary of Huelva. In the case of As, the mean concentration exceeded the European annual target value in PM_{10} (6 ng m^{-3}, European Commission, 2004), which will become a limit value from January 1st, 2030 (European Union, 2024). However, other works carried out at this station (e.g., Millán-Martínez et al., 2021a) showed a higher concentration of the As species with a lower harmful effect on health. The target value of Cd (5 ng m^{-3}, European Commission, 2004) and the limit value of Pb (500 ng m^{-3}, European Commission, 1999), were not exceeded. The Campus and Moguer sites are also influenced by the emissions of this smelter (e.g., Pérez-Vizcaíno et al., 2025), although the measured concentrations were lower. In the case of Zn, the highest concentration was measured at the Lepanto site (81.2 ng m^{-3}), associated with emissions from smelters located near the city of Córdoba (de la Rosa et al., 2010). However, in the stations of La Rábida, Campus and Moguer, Zn concentrations were also high and related to the copper smelter of Huelva.

The urban-industrial station of Bailén registered the highest concentration of V (24.9 ng m^{-3}) and Rb (2.1 ng m^{-3}). The first is associated with emissions from the combustion of coke in the numerous local brick factories (Sánchez de la Campa and de la Rosa, 2014), while the second is related to the combustion of olive husk (Sánchez de la Campa et al., 2010). The two sites with the highest mean values of Cr and Ni were the urban-industrial stations of La Línea (14.9 ng m^{-3} and 10.4 ng m^{-3}, respectively) and Puente Mayorga (11.1 ng m^{-3} and 9.2 ng m^{-3}, respectively). Nevertheless, Ni levels were lower than the annual target value of 20 ng m^{-3} (European Commission, 2004). These elevated Cr values and a V/Ni ratio between 0.5 and 0.6 for the three stations in the Bay of Algeciras (La Línea, Los Barrios and Puente Mayorga) suggest a significant influence from the stainless-steel manufacturing plant located in that area (Moreno et al., 2010; Pandolfi et al., 2011).

Finally, the highest mean concentrations of Sn and Sb were measured at the Granada Norte (4.0 ng m^{-3} and 1.9 ng m^{-3}, respectively) and Torneo (4.6 ng m^{-3} and 2.1 ng m^{-3}, respectively) traffic sites. In urban environments, these elements are associated with vehicle brake wear (Amato et al., 2014; Piscitello et al., 2021).

4.5. Source apportionment

A PMF analysis was performed for the 21 monitoring stations to identify and quantify the sources that contributed to PM_{10} levels during the study period. The results were similar to that obtained by Millán-Martínez et al. (2021b) between 2007 and 2014 in Andalusia. Six sources were recognized: Crustal, Marine, Combustion, Traffic, Regional

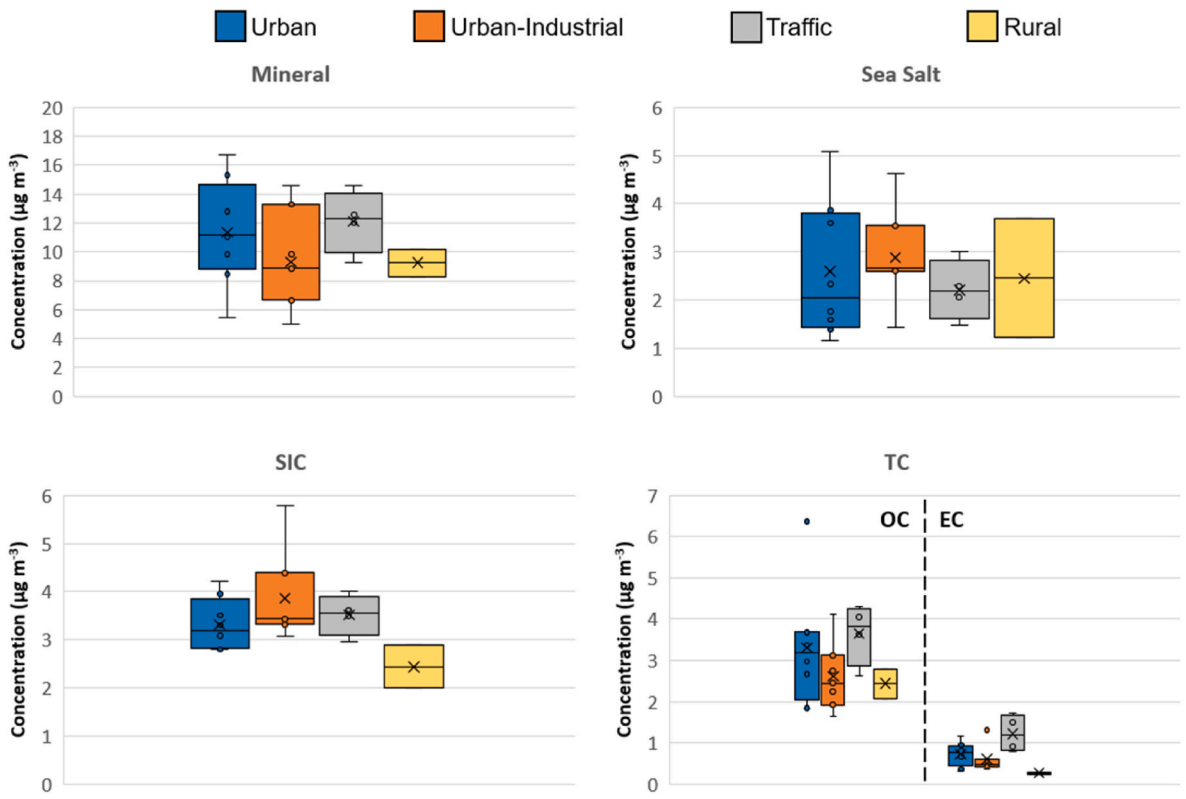

Fig. 3. Box-and-whisker plots of 2021–2023 mean concentrations of the four major components (Mineral, Sea Salt, SIC and TC) between 2021 and 2023 at the monitoring stations.

and Industrial. These sources are also consistent with those identified in southwestern Europe in other studies (e.g., Karagulian et al., 2015; Liu et al., 2025b). Source profiles for each station and the unaccounted concentration can be found in Fig. S3 and Table S7, respectively.

The first source is the Crustal source and it is mainly characterized by Al, Ca, Fe, Mn, Rb, Sr and Ti. These elements are associated with African dust episodes (e.g., Rodríguez et al., 2001) and/or local anthropogenic dust, such as road and construction dust, and soil dust resuspension (e.g., Querol et al., 2001). The concentration of this source is similar (7.3–8.9 µg m^{-3}) in the four groups of stations (Fig. 4), although it represents a higher percentage (41 %) in rural stations due to the lower source contribution of the other sources. The Moguer urban-industrial site was the station with the highest concentration of this source, both including the African dust (12.3 µg m^{-3}) and subtracting it (8.0 µg m^{-3}) (Table 1).

The Marine source is characterized by the typical marine species Cl^-, Mg and Na. These elements are the main constituents of common sea salts (e.g., Fujitani et al., 2007; Cochran et al., 2017). The sites where the Marine source is more relevant are urban-industrial monitoring stations (4.2 µg m^{-3}; 18 %; Fig. 4) due to the influence of sea breeze as most of them are located near the coast (Fig. 1). In some stations (Palacio de Congresos, Villanueva del Arzobispo, Campus and Granada Norte), the sea sprays interact with secondary inorganic aerosols and gaseous precursors such as SO_4^{2-} and NO_3^-, thus corresponding to an 'Aged' Marine source (Fig. S3).

The third source is Combustion and the main associated species are K, Rb, OC and EC. These species are emitted from agricultural processes (e.g., Yin et al., 2023) and domestic biomass burning (e.g., Samara et al., 2014). EC and OC are also emitted by road traffic, but in cities with high biomass burning contributions, they are included in the Combustion source. The concentration of this source ranged between 1.0 and 5.2 µg m^{-3}, with traffic sites having the lowest concentrations (Fig. 4), when the Traffic source is clearly identified. This source accounts for the highest PM_{10} load at rural sites (28 %). The site with the highest Combustion contribution was Villanueva del Arzobispo (11.4 µg m^{-3}; 40 %; Fig. S4).

The Traffic source is characterized by different components (Ba, Ca, Cr, Cu, Fe, K, Sb, Sn, Zn, OC, EC) derived from emissions from vehicle exhaust (e.g., diesel soot), brake and tire wear or road dust (e.g., Amato et al., 2014; Charron et al., 2019; Piscitello et al., 2021). As it could be expected, the concentration and relative contribution of Traffic to PM_{10} reached the highest levels at traffic sites (7.3 µg m^{-3}; 29 %; Fig. 4). Granada Norte reached the highest contribution (10.7 µg m^{-3}; 39 %; Fig. S4), and a traffic source associated with exhaust emissions and another associated with road dust were reported separately at this site (Fig. S3).

The fifth source is Regional. The species are secondary aerosols (NH_4^+, NO_3^- and SO_4^{2-}) generated from gaseous precursors and associated with regional production of SIC and long-range transport (e.g., Viana et al., 2008; Karagulian et al., 2015). NH_4^+ originates from the use of fertilizers and agricultural activities, while NO_3^- and SO_4^{2-} are secondary inorganic aerosols formed from the oxidation of other species (NO_x and SO_2, respectively) emitted in industrial and/or combustion contexts (Liu et al., 2025b). Other elements (V, Ni and Pb) are also included as they correspond to tracers of residual oil combustion emissions such as shipping or power plants (e.g., Pandolfi et al., 2020). The contribution of this source was similar in the four groups of monitoring sites (3.1–4.2 µg m^{-3}; 14–17 %; Fig. 4). The site with the highest concentration was Carranque (9.4 µg m^{-3}; 41 %; Fig. S4).

Finally, the Industrial source is characterized by metals and metalloids such as As, Cd, Cu, Ni, Pb and Zn. These elements are associated with emissions from smelters, oil refineries, industrial power plants and ceramic facilities (e.g., Serbula et al., 2014; Yang et al., 2024), among other types of activities. The highest contribution of this source was measured at urban-industrial sites (3.5 µg m^{-3}; 15 %; Fig. 4). At La Rábida and Campus stations, more than one source associated with

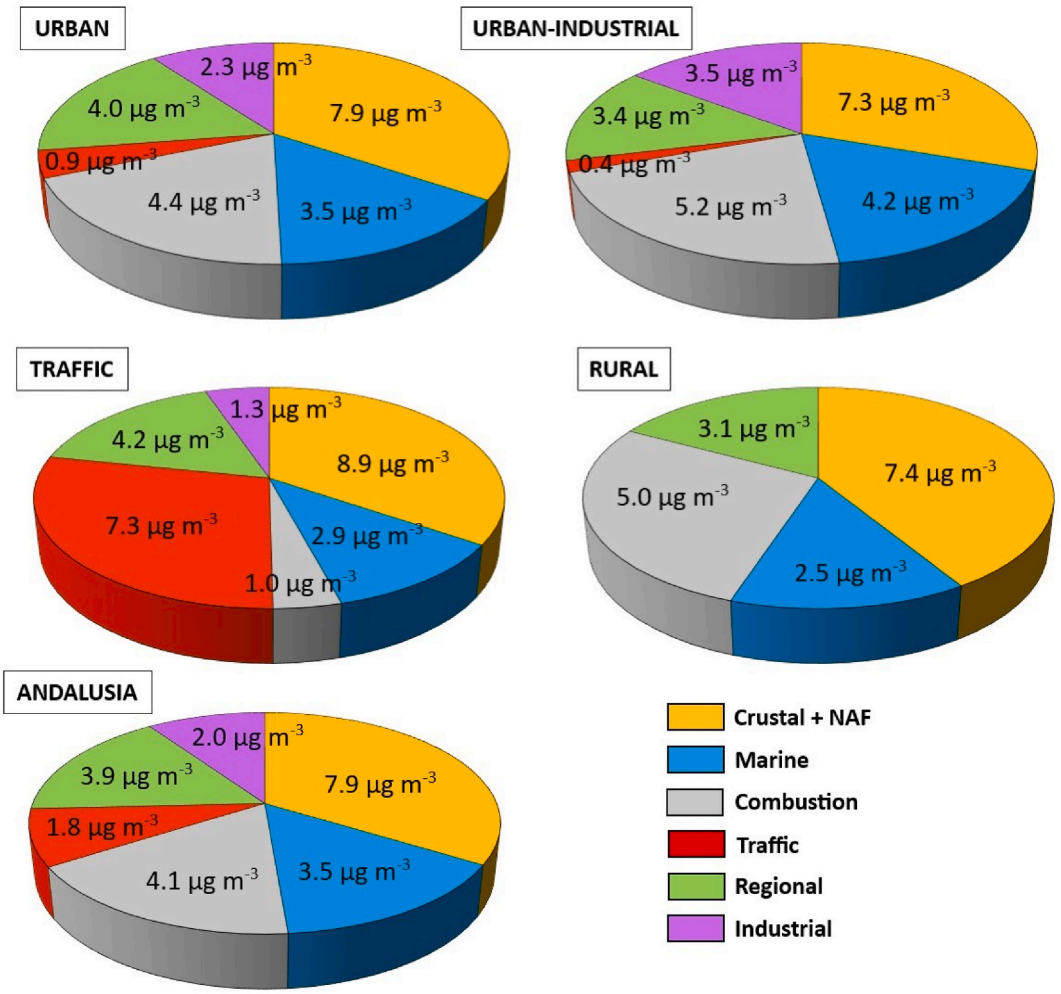

Fig. 4. Pie charts of the mean contributions (µg m^{-3}) of each source to PM_{10} concentration for each group of stations (urban, urban-industrial, traffic and rural) and for all the stations in the study (Andalusia). NAF: North African dust load.

industrial activity were identified (Fig. S3), with the latter showing the highest concentration (5.8 µg m^{-3}; Fig. S4) among all stations in this study.

4.6. Emission reduction strategies for 2030 compliance

To reduce annual PM_{10} levels at the 9/21 air quality monitoring sites that would have exceeded the annual limit value of the Ambient Air Quality Directive (EU) 2024/2881, it is necessary to abate the emissions from the high PM_{10} contribution sources identified (Fig. S5). These emissions come mostly from Traffic, Combustion (biomass burning and traffic mix) and/or Industrial sources. These 9/21 sites were Alcalá de Guadaíra, Villanueva del Arzobispo, Bailén, Campus, La Línea, Moguer, Granada Norte, Príncipes and Torneo stations (Table 1). It should be noted that the contribution of the African dust load may vary annually, so the reduction percentages proposed below correspond to the minimum decrease of each source.

In the case of the Granada Norte traffic site, this decrease should be at least of 5 % the contribution of the Traffic source to the annual PM_{10} mean. However, at Príncipes and Torneo sites in Seville, the reduction should reach around 33 % (Table S8). For these sites, the implementation of LEZs in Granada and Seville including the areas where these sites are located, favoring the modal transport shift from private vehicles to public and active transport, implementing congestion charges, reducing the number of urban freight distribution vehicles, among others, are recommended (MITERD, 2025). In addition, the Regional Government of Andalusia incorporated a qualitative cost-benefit analysis, classifying the measures according to both their economic requirements and their expected emission reduction potential. This socio-economic evaluation provides evidence that strategies such as LEZs and other mitigation strategies are not only environmentally effective but also economically viable and context-appropriate in Andalusian cities.

In the case of urban-industrial and urban background sites, the concentration of the Combustion source should be reduced by 50 % at the Moguer station, and around 15 % at the Villanueva del Arzobispo and Alcalá de Guadaíra urban sites. In the rest of the urban-industrial sites, the reduction should reach 25 % (Campus) and 20 % (Bailén and La Línea) (Table S8). To reduce the concentration of Combustion contribution, agricultural, domestic-commercial and industrial biomass burning will need to be the major abatement target for emissions to reduce PM_{10} concentrations (MITERD, 2025).

The Industrial contribution should be reduced by 50 % at Moguer station, 33 % at Príncipes, 25 % at Campus, 20 % at Bailén and 15 % at Alcalá de Guadaíra (Table S8). To mitigate these emissions, it would be necessary to continue with the implementation of abatement techniques in the ceramic industry of Bailén (focused on the reduction of SO_2 emissions, Sánchez de la Campa and de la Rosa, 2014) and the industrial areas of the Bay of Algeciras and the Estuary of Huelva (such as wet electrofilters and bag filters in the copper production, Sánchez de la Campa et al., 2018).

5. Conclusions

An evaluation of the 2021–2023 PM_{10} concentrations, chemical speciation and receptor modelling source apportionment was carried out using data from 21 air quality monitoring sites throughout Andalusia (southern Spain). The novelty of the study is in the implementation of receptor modelling source apportionment based on the evaluation of long-term PM_{10} speciation datasets to assess on the strategies needed to attain compliance with the PM_{10} standard of the Ambient Air Quality Directive (EU) 2024/2881 to be met from January 1st, 2030.

The source apportionment analysis conducted with PMF recognized six major contributing sources of PM_{10}: Crustal (traced by Al, Ca, Fe, Mn, Rb, Sr and Ti), Marine (Cl^-, Mg and Na), Combustion (K, Rb, OC and EC, a biomass burning and traffic mix), Traffic (Ba, Ca, Cr, Cu, Fe, K, Sb, Sn, Zn, OC and EC), Regional (V, Ni, Pb, NH_4^+, NO_3^- and SO_4^{2-}) and Industrial (As, Cd, Cu, Ni, Pb and Zn).

Nine out of 21 study sites would have exceeded the 2030 limit value for PM_{10} with the concentrations recorded in 2021–2023. Specific emission abatement measures are recommended for each case according to the results of the source apportionment.

Receptor modelling tools do not allow tracing the origin of the gaseous precursors yielding to secondary inorganic and organic PM. To this end, the deterministic models should be used to assess on strategies to abate PM. However, the accuracy of these modelling tools may be lower than that of receptor modelling (starting for measurement data). Accordingly, due to the strictness of the forthcoming air quality standards and the high proportion of secondary PM, it is highly recommended to link the results of deterministic and receptor modelling for obtaining a better accuracy for source apportionment of PM. This would yield in a marked improvement of the accuracy of the assessment for cost-effective measures.

Another step forward would be to combine with high time resolution (i.e., 1-h) PM speciation measurements to provide databases for receptor modelling to have a better knowledge in the variations of the different tracer elements of each source.

CRediT authorship contribution statement

Pablo Pérez-Vizcaíno: Writing – original draft, Investigation, Conceptualization. **Ana M. Sánchez de la Campa:** Writing – review & editing, Methodology. **Daniel Sánchez-Rodas:** Writing – review & editing, Methodology. **Andrés Alastuey:** Writing – review & editing, Methodology. **Xavier Querol:** Writing – review & editing, Methodology. **Jesús D. de la Rosa:** Writing – review & editing, Methodology, Funding acquisition.

Declaration of competing interest

The authors declare the following financial interests/personal relationships which may be considered as potential competing interests: Jesus Damian de la Rosa Diaz reports financial support was provided by Spain Ministry of Science, Innovation and Universities. Pablo Perez Vizcaino reports financial support was provided by Spain Ministry of Science, Innovation and Universities. Pablo Perez Vizcaino reports a relationship with Spain Ministry of Science, Innovation and Universities that includes: funding grants. If there are other authors, they declare that they have no known competing financial interests or personal relationships that could have appeared to influence the work reported in this paper.

Acknowledgments

This study has received funding from the RI-URBANS project, belonging to the European Union's Horizon 2020 research and innovation program (101036245). We would also like to acknowledge Grants PID2021-126986OB-I00 (Ref. PRE2022-105241) and PID2024-157355OB-I00 funded by MCIN/AEI/10.13039/501100011033 and, by "ERDF A way of making Europe", and the Consejería de Universidad, Investigación e Innovación (Ref. DGP_PIDI_2024_01602) of the Regional Government of Andalusia for financial and technical support. Funding for open access charge: University of Huelva/CBUA.

Appendix A. Supplementary data

Supplementary data to this article can be found online at https://doi.org/10.1016/j.envpol.2025.127347.

Data availability

Data will be made available on request.

References

Alastuey, A., Querol, X., Plana, F., Viana, M., Ruiz, C.R., Sánchez de la Campa, A., de la Rosa, J., Mantilla, E., García dos Santos, S., 2006. Identification and chemical characterization of industrial PM sources in SW Spain. Journal of Air Waste Management 56, 993–1006. https://doi.org/10.1080/10473289.2006.10464502.

Amato, F., Alastuey, A., de la Rosa, J., González Castanedo, Y., Sánchez de la Campa, A. M., Pandolfi, M., Lozano, A., Contreras González, J., Querol, X., 2014. Trends of road dust emissions contributions on ambient air particulate levels at rural, urban and industrial sites in southern Spain. Atmos. Chem. Phys. 14, 3533–3544. https://doi.org/10.5194/acp-14-3533-2014.

Belis, C., Favez, O., Mircea, M., Diapouli, E., Manousakas, M., Vratolis, S., Gilardoni, S., Paglione, M., Decesari, S., Mocnik, G., Mooibroek, D., Salvador, P., Takahama, S., Vecchi, R., Paatero, P., 2019. European guide on air pollution source apportionment with receptor models. Joint Research Centre reference reports EUR26080 EN. https://doi.org/10.2760/439106.

Beloconi, A., Vounatsou, P., 2023. Revised EU and WHO air quality thresholds: where does Europe stand? Atmos. Environ. 314, 120110. https://doi.org/10.1016/j.atmosenv.2023.120110.

Cavalli, F., Viana, M., Yttri, K.E., Genberg, J., Putaud, J.-P., 2010. Toward a standarised thermal-optical protocol for measuring atmospheric organic and elemental carbon: the EUSAAR protocol. Atmos. Meas. Tech. 3, 79–89. https://doi.org/10.5194/amt-3-79-2010.

Cesari, D., Amato, F., Pandolfi, M., Alastuey, A., Querol, X., Contini, D., 2016a. An inter-comparison of PM_{10} source apportionment using PCA and PM receptor models in three European sites. Environ. Sci. Pollut. Control Ser. 23, 15133–15148. https://doi.org/10.1007/s11356-016-6599-z.

Cesari, D., Donateo, A., Conte, M., Contini, D., 2016b. Inter-comparison of source apportionment of PM_{10} using PMF and CMB in three sites nearby an industrial area in central Italy. Atmos. Res. 182, 282–293. https://doi.org/10.1016/j.atmosres.2016.08.003.

Charron, A., Polo-Rehn, L., Besomber, J.-L., Golly, B., Buisson, C., Chanut, H., Marchand, N., Guillaud, G., Jaffrezo, J.-L., 2019. Identification and quantification of particulate tracers of exhaust and non-exhaust vehicle emissions. Atmos. Chem. Phys. 19, 5187–5207. https://doi.org/10.5194/acp-19-5187-2019.

Chowdhury, C., Pozzer, A., Haines, A., Klingmüller, K., Münzel, T., Paasonen, P., Sharma, A., Venkataraman, C., Lelieveld, J., 2022. Global health burden of ambient $PM_{2.5}$ and the contribution of anthropogenic black carbon and organic aerosols. Environ. Int. 159, 107020. https://doi.org/10.1016/j.envint.2021.107020.

Clemente, Á., Yubero, E., Galindo, N., Crespo, J., Nicolás, J.F., Santacatalina, M., Carratala, A., 2021. Quantification of the impact of port activities on PM_{10} levels at the port-city boundary of a mediterranean city. J. Environ. Manag. 281, 111842. https://doi.org/10.1016/j.jenvman.2020.111842.

Cochran, R.E., Ryder, O.S., Grassian, V.H., Prather, K.A., 2017. Sea spray aerosol: the chemical link between the Oceans, atmosphere and climate. Accounts of Chemical Research 50, 599–604. https://doi.org/10.1021/acs.accounts.6b00603.

Cuevas-Agulló, E., Barriopedro, D., García, R.D., Alonso-Pérez, S., González-Alemán, J.J., Werner, E., Suárez, D., Bustos, J.J., García-Castrillo, G., García, O., Barreto, Á., Basart, S., 2024. Sharp increase in Saharan dust intrusions over the western Euro-Mediterranean in February-March 2020-2022 and associated atmospheric circulation. Atmos. Chem. Phys. 24, 4083–4104. https://doi.org/10.5194/acp-24-4083-2024.

de la Rosa, J.D., Sánchez de la Campa, A.M., Alastuey, A., Querol, X., González-Castanedo, Y., Fernández-Camacho, R., Stein, A.F., 2010. Using PM_{10} geochemical maps for defining the origin of atmospheric pollution in Andalusia (Southern Spain). Atmos. Environ. 44, 4595–4605. https://doi.org/10.1016/j.atmosenv.2010.08.009.

Escudero, M., Querol, X., Pey, J., Alastuey, A., Pérez, N., Ferreira, F., Alonso, S., Rodríguez, S., Cuevas, E., 2007. A methodology for the quantification of the net African dust load in air quality monitoring networks. Atmos. Environ. 41, 5516–5524. https://doi.org/10.1016/j.atmosenv.2007.04.047.

European Commission, 1999. Directive 1999/30/EC of the Council directive of 22/04/1999 relating to limit values for sulphur dioxide, nitrogen dioxide and oxides of nitrogen, particulate matter and lead in ambient air. https://n9.cl/lcv6iq (accessed January 2025).

European Commission, 2004. Directive 2004/107/EC of the European Parliament and of the Council of 15/12/2004 relating to arsenic, cadmium, mercury, nickel and

polycyclic aromatic hydrocarbons in ambient air. https://n9.cl/k7uo4 (accessed January 2025).
European Commission, 2008. Directive 2008/50/EC of the European Parliament and of the Council of 21/05/2008 on ambient air quality and cleaner air for Europe. https://n9.cl/ecxs2f (accessed January 2025).
European Commission, 2011. Commission staff working paper establishing guidelines for demonstration and subtraction of exceedances attributable to natural sources under the Directive 2008/50/EC on ambient air quality and cleaner air for Europe. https://n9.cl/x9ils (accessed July 2025).
European Environment Agency, 2024. ETC HE Report 2023/3: air quality maps of EEA member and cooperating countries for 2021. PM10, PM2.5, O3, NO2, Nox and BaP spatial estimates and their uncertainties. https://n9.cl/lbgf6 (accessed June 2025).
European Union, 2024. Directive (EU) 2024/2881 of the European Parliament and of the Council of 23/10/2024 on ambient air quality and cleaner air for Europe. https://n9.cl/9vums (accessed January 2025).
Fernández-Camacho, R., de la Rosa, J., Sánchez de la Campa, A.M., González-Castanedo, Y., Alastuey, A., Querol, X., Rodríguez, S., 2010. Geochemical characterization of Cu-smelter emission plumes with impact in an urban area of SW Spain. Atmos. Res. 96, 590–601. https://doi.org/10.1016/j.atmosres.2010.01.008.
Fernández-Camacho, R., de la Rosa, J.D., Sánchez de la Campa, A.M., 2016. Trends and sources vs air mass origins in a major city in South-western Europe: implications for air quality management. Sci. Total Environ. 553, 305–315. https://doi.org/10.1016/j.scitotenv.2016.02.079.
Fujitani, Y., Murao, N., Ohta, S., Endoh, T., Yamagata, S., 2007. Optical and chemical properties of marine aerosols over the central equatorial Pacific Ocean during the 2003 R/V Mirai cruise. J. Geophys. Res. 112, D11213. https://doi.org/10.1029/2006JD008354.
Gu, J., Deffner, V., Küchenhoff, H., Pickford, R., Breitner, S., Schneider, A., Kowalski, M., Petters, A., Lutz, M., Kerschbaumer, A., Slama, R., Morelli, X., Wichmann, H.-E., Cyrys, J., 2022. Low emission zones reduced PM_{10} but not NO_2 concentrations in Berlin and Munich, Germany. J. Environ. Manag. 302, 114048. https://doi.org/10.1016/j.jenvman.2021.114048.
Gupta, I., Salunkhe, A., Kumar, R., 2012. Source apportionment of PM_{10} by positive matrix factorization in urban area of Mumbai, India. Sci. World J. 2012, 585791. https://doi.org/10.1100/2012/585791.
Holman, C., Harrison, R., Querol, X., 2015. Review of the efficacy of low emission zones to improve urban air quality in European cities. Atmos. Environ. 111, 161–169. https://doi.org/10.1016/j.atmosenv.2015.04.009.
in 't Veld, M., Alastuey, A., Pandolfi, M., Amato, F., Pérez, N., Reche, C., Via, M., Minguillón, M.C., Escudero, M., Querol, X., 2021. Compositional changes of $PM_{2.5}$ in NE Spain during 2009-2018: a trend analysis of the chemical composition and source apportionment. Sci. Total Environ. 795, 148728. https://doi.org/10.1016/j.scitotenv.2021.148728.
Jo, E.-J., Lee, W.-S., Jo, H.-Y., Kim, C.-H., Eom, J.-S., Mok, J.-H., Kim, M.-H., Lee, K., Kim, K.-U., Lee, M.-K., Park, H.-K., 2017. Effects of particulate matter on respiratory disease and the impact of meteorological factors in Busan, Korea. Respir. Med. 124, 79–87. https://doi.org/10.1016/j.rmed.2017.02.010.
Karagulian, F., Belis, C.A., Dora, C.F.C., Prüss-Ustün, A.M., Bonjour, S., Adair-Rohani, H., Amann, M., 2015. Contributions to cities' ambient particulate matter (PM): a systemic review of local source contributions at global levels. Atmos. Environ. 120, 475–483. https://doi.org/10.1016/j.atmosenv.2015.08.087.
Li, J., Chen, B., Sánchez de la Campa, A.M., Alastuey, A., Querol, X., de la Rosa, J.D., 2018. 2005-2014 trends of PM10 source contributions in an industrialized area of southern Spain. Environ. Pollut. 236, 570–589. https://doi.org/10.1016/j.envpol.2018.01.101.
Liu, X., Zhang, X., Jin, B., Wang, T., Qian, S., Zou, J., Dinh, V.N.T., Jaffrezo, J.-L., Uzu, G., Dominutti, P., Darfeuil, S., Favez, O., Conil, S., Marchand, N., Castillo, S., de la Rosa, J.D., Grange, S., Hueglin, C., Eleftheriadis, K., Diapouli, E., Manousakas, M.-I., Gini, M., Nava, S., Calzolai, G., Alves, C., Monge, M., Reche, C., Harrison, R.M., Hopke, P.K., Alastuey, A., Querol, X., 2025b. Source apportionment of PM_{10} based on offline chemical speciation data at 24 European sites. npj Clim. Atmos. Sci. 8, 255. https://doi.org/10.1038/s41612-025-01097-7.
Liu, Y., Jin, B., Zhang, X., Liu, X., Wang, T., Dinh, V.N.T., Jaffrezo, J.-L., Uzu, G., Dominutti, P., Darfeuil, S., Favez, O., Conil, S., Marchand, N., Castillo, S., de la Rosa, J.D., Grange, S., Hueglin, C., Eleftheriadis, K., Diapouli, E., Manousakas, M.-I., Gini, M., Calzolai, G., Alves, C., Monge, M., Reche, C., Harrison, R.M., Hopke, P.K., Alastuey, A., Querol, X., 2025a. Source apportionment of PM_{10} particles in the urban atmosphere using PMF and LPO-XGBoost. Environ. Res. 278, 121659. https://doi.org/10.1016/j.envres.2025.121659.
López-Quirós, A., Barbier, M., Martín, J.M., Puga-Bernabéu, A., Guichet, X., 2016. Diagenetic evolution of Tortonian temperate carbonates close to evaporites in the Granada Basin (SE Spain). Sediment. Geol. 335, 180–196. https://doi.org/10.1016/j.sedgeo.2016.02.011.
Marquès, M., Correig, E., Ibarretxe, D., Anoro, E., Arroyo, J.A., Jericó, C., Borrallo, R.M., Miret, M., Näf, S., Pardo, A., Perea, V., Pérez-Bernalte, R., Ramírez-Montesinos, R., Royuela, M., Soler, C., Urquizu-Padill, a M., Zamora, A., Pedro-Botet, J., , on behalf of the STACOV-XULA research group, Masana, L., Domingo, J.L., 2022. Long-term exposure to PM_{10} above WHO guidelines exacerbates COVD-10 severity and mortality. Environ. Int. 158, 106930. https://doi.org/10.1016/j.envint.2021.106930.
Martinelli, N., Olivieri, O., Girelli, D., 2013. Air particulate matter and cardiovascular disease: a narrative review. Eur. J. Intern. Med. 24, 295–302. https://doi.org/10.1016/j.ejim.2013.04.001.
Mebrahtu, T.F., Santorelli, G., Yang, T.C., Wright, J., Tate, J., McEachan, R.R.C., 2023. The effects of exposure to NO_2, $PM_{2.5}$ and PM_{10} on health service attendances with respiratory illnesses: a time-series analysis. Envirommental Pollution 333, 122123. https://doi.org/10.1016/j.envpol.2023.122123.
Millán-Martínez, M., Sánchez-Rodas, D., Sánchez de la Campa, A.M., Alastuey, A., Querol, X., de la Rosa, J.D., 2021a. Source contribution and origin of PM10 and arsenic in a complex industrial region (Huelva, SW Spain). Environ. Pollut. 274, 116268. https://doi.org/10.1016/j.envpol.2020.116268.
Millán-Martínez, M., Sánchez-Rodas, D., Sánchez de la Campa, A.M., de la Rosa, J.D., 2021b. Contribution of anthropogenic and natural sources in PM10 during North African dust events in Southern Europe. Environ. Pollut. 290, 118065. https://doi.org/10.1016/j.envpol.2021.118065.
MITERD, 2025. Guía para la elaboración de planes de mejora de la calidad del aire. Ministerio Para la Transición Ecológica Y El Reto Demográfico, p. 180. https://n9.cl/d70kw (accessed July 2025).
Moreno, T., Querol, X., Alastuey, A., Viana, M., Salvador, P., Sánchez de la Campa, A., Artiñano, B., de la Rosa, J., Gibbons, W., 2006. Variations in atmospheric PM trace metal content in Spanish towns: illustrating the chemical complexity of the inorganic urban aerosol cocktail. Atmos. Environ. 40, 6791–6803. https://doi.org/10.1016/j.atmosenv.2006.05.074.
Moreno, T., Querol, X., Alastuey, A., de la Rosa, J., Sánchez de la Campa, A.M., Minguillón, M., Pandolfi, M., González-Castanedo, Y., Monfort, E., Gibbons, W., 2010. Variations in vanadium, nickel and lanthanoid element concentrations in urban air. Sci. Total Environ. 408, 4569–4579. https://doi.org/10.1016/j.scitotenv.2010.06.016.
Neuberger, M., Schimek, M.G., Horak Jr, F., Moshammer, H., Kundi, M., Frischer, T., Gomiscek, B., Puxbaum, H., Hauck, H., AUPHEP-Team, 2004. Acute effects of particulate matter on respiratory diseases, symptoms and functions: epidemiological results of the Austrian Project on Health Effects of Particulate Matter (AUPHEP). Atmos. Environ. 38, 3971–3981. https://doi.org/10.1016/j.atmosenv.2003.12.044.
Paatero, P., Tapper, U., 1994. Positive matrix factorization: a nonnegative factor model with optimal utilization of error estimates of data values. Environmetrics 5, 111–126. https://doi.org/10.1002/env.3170050203.
Paatero, P., 1997. Least square formulation of robust non-negative factor analysis. Chemometr. Intell. Lab. Syst. 3, 23–35. https://doi.org/10.1016/S0169-7439(96)00044-5.
Paatero, P., Hopke, P.K., 2003. Discarding or downweighting high-noise variables in factor analytic models. Anal. Chim. Acta 490, 277–289. https://doi.org/10.1016/S0003-2670(02)01643-4.
Pandolfi, M., Gonzalez-Castanedo, Y., Alastuey, A., de la Rosa, J.D., Mantilla, E., Sánchez de la Campa, A., Querol, X., Pey, J., Amato, F., Moreno, T., 2011. Source apportionment of PM_{10} and $PM_{2.5}$ at multiple sites in the strait of Gibraltar by PMF: impact of shipping emissions. Environ. Sci. Pollut. Control Ser. 18, 260–269. https://doi.org/10.1007/s11356-010-0373-4.
Pandolfi, M., Mooibroek, D., Hopke, P., van Pinxteren, D., Querol, X., Herrmann, H., Alastuey, A., Favez, O., Hüglin, C., Perdrix, E., Riffault, V., Sauvage, S., van der Swaluw, E., Tarasova, O., Colette, A., 2020. Long-range and local air pollution: what can we learn from chemical speciation or particulate matter at paired sites? Atmos. Chem. Phys. 20, 409–429. https://doi.org/10.5194/acp-20-409-2020.
Pérez, N., Pey, J., Reche, C., Cortés, J., Alastuey, A., Querol, X., 2016. Impact of harbour emissions on ambient PM_{10} and $PM_{2.5}$ in Barcelona (Spain): evidences of secondary aerosol formation within the urban area. Sci. Total Environ. 571, 237–250. https://doi.org/10.1016/j.scitotenv.2016.07.025.
Pérez-Pastor, R., Salvador, P., García-Alonso, S., Alastuey, A., García dos Santos, S., Querol, X., Artíñano, B., 2020. Characterization of organic aerosol at a rural site influenced by olive waste biomass burning. Chemosphere 248, 125896. https://doi.org/10.1016/j.chemosphere.2020.125896.
Pérez-Vizcaíno, P., Sánchez de la Campa, A.M., Sánchez-Rodas, D., de la Rosa, J.D., 2025. Application of a near real-time technique for the assessment of atmospheric arsenic and metals emissions from a copper smelter in an urban area of SW Europe. Environ. Pollut. 367, 125602. https://doi.org/10.1016/j.envpol.2024.125602.
Peters, A., 2005. Particulate matter and heart disease: evidence from epidemiological studies. Toxicol. Appl. Pharmacol. 207, S477–S482. https://doi.org/10.1016/j.taap.2005.04.030.
Piscitello, A., Bianco, C., Casasso, A., Sethi, R., 2021. Non-exhaust traffic emissions: sources, characterization, and mitigation measures. Sci. Total Environ. 766, 144440. https://doi.org/10.1016/j.scitotenv.2020.144440.
Polichetti, G., Cocco, S., Spinali, A., Trimarco, V., Nunziata, A., 2009. Effects of particulate matter (PM_{10}, $PM_{2.5}$ and PM_1) on the cardiovascular system. Toxicology 261, 1–8. https://doi.org/10.1016/j.tox.2009.04.035.
Querol, X., Alastuey, A., Rodríguez, S., Plana, F., Ruiz, C.R., Cots, N., Massagué, G., Puig, O., 2001. PM10 and PM2.5 source apportionment in the Barcelona Metropolitan area, Catalonia, Spain. Atmos. Environ. 35, 6407–6419. https://doi.org/10.1016/S1352-2310(01)00361-2.
Querol, X., Alastuey, A., de la Rosa, J., Sánchez de la Campa, A., Plana, F., Ruiz, C.R., 2002. Source apportionment analysis of atmospheric particulates in an industrialized urban site in southwestern Spain. Atmos. Environ. 36, 3113–3125. https://doi.org/10.1016/S1352-2310(02)00257-1.
Querol, X., Alastuey, A., Pandolfi, M., Reche, C., Pérez, N., Minguillón, M.C., Moreno, T., Viana, M., Escudero, M., Orio, A., Pallarés, M., Reina, F., 2014. 2001-2012 trends on air quality in Spain. Sci. Total Environ. 490, 957–969. https://doi.org/10.1016/j.scitotenv.2014.05.074.
Querol, X., Pérez, N., Reche, C., Ealo, M., Ripoll, A., Tur, J., Pandolfi, M., Pey, J., Salvador, P., Moreno, T., Alastuey, A., 2019. African dust and air quality over Spain: is it only dust that matters? Sci. Total Environ. 686, 737–752. https://doi.org/10.1016/j.scitotenv.2019.05.349.

RI-URBANS, 2025. Guidance Documents on Measurements and Modelling of Novel Air Quality Pollutants in Urban Europe: Summary and Added Value. RI-URBANS, p. 66. H2020 project (10103624). https://n9.cl/xuhed (accessed July 2025).

RI-URBANS-ST10, 2025. Guidance documents on measurements and modelling of novel air quality pollutants: source apportionment Techniques for PM. RI-URBANS. H2020 project (10103624) 51. https://n9.cl/zb33b (accessed July 2025).

Rodríguez, S., Querol, X., Alastuey, A., Kallos, G., Kakaliagou, O., 2001. Saharan dust contributions to PM10 and TSP levels in Southern and Eastern Spain. Atmos. Environ. 35, 2433–2447. https://doi.org/10.1016/S1352-2310(00)00496-9.

Rodríguez, S., López-Darias, J., 2024. Emerging extreme Saharan-dust events expand northward over the Atlantic and Europe prompting record-breaking PM_{10} and $PM_{2.5}$ episodes. Atmos. Chem. Phys. 24, 12031–12053. https://doi.org/10.5194/acp-24-12031-2024.

Salvador, P., Pey, J., Pérez, N., Querol, X., Artíñano, B., 2022. Increasing atmospheric dust transport towards the western Mediterranean over 1948-2020. npj Clim. Atmos. Sci. 5, 34. https://doi.org/10.1038/s41612-022-00256-4.

Samara, C., Voutsa, D., Kouras, A., Eleftheriadis, K., Maggos, T., Saraga, D., Petrakakis, M., 2014. Organic and elemental carbon associated to PM_{10} and $PM_{2.5}$ at urban sites of northern Greece. Environ. Sci. Pollut. Control Ser. 21, 1769–1785. https://doi.org/10.1007/s11356-013-2052-8.

Sánchez de la Campa, A.M., de la Rosa, J.D., González-Castanedo, Y., Fernández-Camacho, R., Alastuey, A., Querol, X., Pio, C., 2010. High concentrations of heavy metals in PM from ceramic factories of Southern Spain. Atmos. Res. 96, 633–644. https://doi.org/10.1016/j.atmosres.2010.02.011.

Sánchez de la Campa, A.M., de la Rosa, J.D., 2014. Implications for air quality and the impact of financial and economic crisis in South Spain: geochemical evolution of atmospheric aerosol in the ceramic region of Bailén. Atmos. Environ. 98, 519–529. https://doi.org/10.1016/j.atmosenv.2014.09.023.

Sánchez de la Campa, A.M., Sánchez-Rodas, D., Alsioufi, L., Alastuey, A., Querol, X., de la Rosa, J.D., 2018. Air quality trends in an industrialized area of SW Spain. J. Clean. Prod. 186, 465–474. https://doi.org/10.1016/j.jclepro.2018.03.122.

Santos, F.M., Gómez-Losada, A., Pires, J.C.M., 2019. Impact of the implementation of Lisbon low emission zone on air quality. J. Hazard Mater. 365, 632–641. https://doi.org/10.1016/j.jhazmat.2018.11.061.

Serbula, S.M., Ilic, A.A., Kalinovic, J.V., Kalinovic, T.S., Petrovic, N.B., 2014. Assessment of air pollution originating from copper smelter in Bor (Serbia). Environ. Earth Sci. 71, 1651–1661. https://doi.org/10.1007/s12665-013-2569-7.

Sharma, S.K., Mandal, T.K., Saxena, M., Rashmi, Rohtash, Sharma, A., Gautam, R., 2014. Source apportionment of PM_{10} by using positive matrix factorization at an urban site of Delhi, India. Urban Clim. 10, 656–670. https://doi.org/10.1016/j.uclim.2013.11.002.

UNE-EN 12341, 2024. Ambient Air - Standard Gravimetric Measurement Method for the Determination of the PM10 or PM2.5 Mass Concentration of Suspended Particulate Matter.

Viana, M., Kuhlbusch, T.A.J., Querol, X., Alastuey, A., Harrison, R.M., Hopke, P.K., Winiwarter, W., Vallius, M., Szidat, S., Prévôt, A.S.H., Hueglin, C., Bloemen, H., Wåhlin, P., Vecchi, R., Miranda, A.I., Kasper-Giebl, A., Maenhaut, W., Hitzenberger, R., 2008. Source apportionment of particulate matter in Europe: a review of methods and results. Aerosol Science 39, 827–849. https://doi.org/10.1016/j.jaerosci.2008.05.007.

Weinmayr, G., Romeo, E., De Sario, M., Weiland, S.K., Forastiere, F., 2010. Short-Term effects of PM_{10} and NO_2 on respiratory health among children with asthma or asthma-like symptoms: a systematic review and meta-analysis. Environ. Health Perspect. 118, 449–457. https://doi.org/10.1289/ehp.0900844.

World Health Organization, 2021. WHO Global Air Quality Guidelines. Particulate Matter ($PM_{2.5}$ and PM_{10}), Ozone, Nitrogen Dioxide, Sulfur Dioxide and Carbon Monoxide. World Health Organization, p. 300. https://n9.cl/iwl94k. accessed January 2025.

Yang, Q., Liu, G., Falandysz, J., Yang, L., Zhao, C., Chen, C., Sun, Y., Zheng, M., Jiang, G., 2024. Atmospheric emissions of particulate matter-bound heavy metals from industrial sources. Sci. Total Environ. 947, 174467. https://doi.org/10.1016/j.scitotenv.2024.174467.

Yin, J., Li, D., Yu, J., Bai, X., Cui, W., Liu, R., Zhuang, M., 2023. Environmental and economic benefits of substituting chemical potassium fertilizer with crop straw residues in China. Environ. Sci. Pollut. Control Ser. 30, 30603–30611. https://doi.org/10.1007/s11356-022-24128-9.

Zhai, M., Wolff, H., 2021. Air pollution and urban road transport: evidence from the world's largest low-emission zone in London. Environ. Econ. Pol. Stud. 23, 721–748. https://doi.org/10.1007/s10018-021-00307-9.

Zheng, B., Tong, D., Li, M., Liu, F., Hong, C., Geng, G., Li, H., Li, X., Peng, L., Qi, J., Yan, L., Zhang, Y., Zhao, H., Zheng, Y., He, K., 2018. Trend in china's anthropogenic emissions since 2010 as the consequence of clean air actions. Atmos. Chem. Phys. 18, 14095–14111. https://doi.org/10.5194/acp-18-14095-2018.